Rheologica Acta (2022) 61:681–688
https://doi.org/10.1007/s00397-022-01355-y

ORIGINAL CONTRIBUTION

Terminal relaxation behavior of entangled linear polymers blended with ring and dumbbell-shaped polymers in melts

Yuya Doi[1,2] · Atsushi Takano[1] · Yoshiaki Takahashi[3] · Yushu Matsushita[1,4]

Received: 24 January 2022 / Revised: 6 June 2022 / Accepted: 6 June 2022 / Published online: 20 June 2022

Abstract

We investigated the terminal relaxation behavior of entangled linear polystyrene L430 (with the entanglement number $Z = M/M_e \simeq 24$, where M is the molecular weight and M_e is the entanglement molecular weight) blended with ring R30 ($M_R \simeq 1.8\ M_e$) and dumbbell-shaped D308030 ($M_R \simeq 1.8\ M_e$ and $M_L \simeq 4.7\ M_e$) polymers. The L430/R30 blend exhibits a one-step relaxation unlike binary linear polymer blends with different molecular weights. The zero-shear viscosity η_0 of the L430/R30 blend is slightly lower than that of the neat L430. These results suggest that spontaneous penetration of the linear chains into the rings occurs, but the rings do not act as entanglement cross-linkers. The L430/D308030 blend also exhibits a one-step relaxation, but its terminal relaxation is slower and broader than that for L430. This result is probably because two ring sections in D308030 are penetrated by the linear chains, and hence D308030 acts as a pseudo-entanglement point with longer characteristic time.

Keywords Terminal relaxation · Entanglement · Ring/linear polymer blends · Dumbbell-shaped polymers

Introduction

Ring polymers are one of the essential model polymers for studying physical properties because they have no chain ends in their structure. In particular, the dynamics of ring polymers is still one of the unsolved and extensively researched topics (Kapnistos et al. 2008; Doi et al. 2015a, 2017; Richter et al. 2015; Vlassopoulos 2016; Kruteva et al. 2020a; Doi 2022). The current understanding is that highly purified ring polymer melts fractionated by liquid chromatography methods (Lee et al. 2000) exhibit viscoelastic behavior similar to that of Rouse ring models at low molecular weights M (Doi et al. 2015a), while at high M, they exhibit a power-law stress relaxation (Kapnistos et al. 2008; Doi et al. 2017). The latter is distinctly different from relaxation behavior for entangled linear and branched polymers (Vlassopoulos 2016). This characteristic molecular dynamic is associated with a more compact conformation of ring polymers in melts than ideal Gaussian ring chains (Suzuki et al. 2009; Halverson et al. 2011; Iwamoto et al. 2018a; Kruteva et al. 2020b). Several molecular models (Obukhov et al. 1994; Ge et al. 2016) have been proposed to describe the dynamics of high-M rings, however, they are not fully understood yet.

Another characteristic property of ring polymers is found in ring/linear polymer blends. Namely, the addition of linear polymers to rings results in spontaneous penetration of the linear chains into the ring molecule, as confirmed by neutron scattering experiments (Iwamoto et al. 2018b) and simulations (Iyer et al. 2007; Subramanian and Shanbhag 2008; Halverson et al. 2012; Tsalikis and Mavrantzas 2014, 2020; Hagita and Murashima 2021). Due to the penetration, the dynamics of ring/linear blends becomes slower than that of pure rings and sometimes even of linear samples, as confirmed with rheological (Kapnistos et al. 2008; Parisi et al. 2020), diffusion (Nam et al. 2009; Kruteva et al. 2017), and spin-echo (Goossen et al. 2015) measurements. In fact, Parisi et al. (2020)

✉ Yuya Doi
ydoi@mp.pse.nagoya-u.ac.jp

✉ Atsushi Takano
atakano@chemibio.nagoya-u.ac.jp

[1] Department of Molecular and Macromolecular Chemistry, Nagoya University, Nagoya 4648603, Japan

[2] Department of Materials Physics, Nagoya University, Nagoya 4648603, Japan

[3] Institute of Materials Chemistry and Engineering, Kyushu University, Kasuga, Fukuoka 8168580, Japan

[4] Toyota Physical and Chemical Research Institute, Nagakute, Aichi 4801192, Japan

proposed that, especially when the fraction of rings is relatively low (≤ 0.3), rings trapped by the multiple threading of linear chains can only relax by linear-chain-induced constraint release (CR) with much slower relaxation than that of the linear chains. Not only the synthetic polymers, but also ring and linear DNAs are used as model polymers to understand their dynamics (Robertson and Smith 2007; Kong et al. 2022). The ring/linear polymer blends also exhibit a peculiar nonlinearity in rheology (Zhou et al. 2019, 2021; Borger et al. 2020; Young et al. 2021). However, there are still few systematic experimental studies on dynamics of ring/linear blends. In particular, in the case of ring/linear blends, the ring/linear molecular weight ratio and the ring/linear mixing ratio need to be considered as parameters of the sample. In many previous rheological studies on ring/linear blends (Kapnistos et al. 2008; Parisi et al. 2020; Kong et al. 2022), ring and linear molecules have the same M being sufficiently higher than the entanglement molecular weight M_e. On the other hand, as the molecular weight of ring polymers M_R becomes lower, it is expected that the number of linear chains which can penetrate into the ring decreases, and eventually the linear chains do not penetrate into the ring. As one of the subjects of this report, we focus on the viscoelasticity of samples blended with well-entangled linear polymers ($M_L \gg M_e$) and rings with relatively low molecular weight ($M_R \simeq 1.8\ M_e$).

Inspired by the dynamics of ring/linear polymer blends, there are several studies on the dynamics of ring polymer derivatives, where ring and linear chains are covalently connected (Doi et al. 2015b, 2020, 2021; Doi 2022). In single-tail tadpole-shaped polystyrene (PS) samples, where a ring ($M_R \simeq 1.8\ M_e$ or $3.3\ M_e$) is connected to one end of a linear chain ($M_L \simeq 1.5 \sim 6.7\ M_e$), the linear tail spontaneously penetrates into the ring part and exhibits a slower terminal relaxation than the individual linear and ring polymers and even the ring/linear polymer blends (Doi et al. 2015b, 2020). In addition, in dumbbell-shaped PS samples, where rings ($M_R \simeq 1.8\ M_e$) were connected to both ends of a linear chain ($M_L \simeq 6.7\ M_e$ and $14\ M_e$), one dumbbell chain spontaneously penetrates into the ring part of another dumbbell molecule, forming a unique penetration/entanglement network with a remarkably slow relaxation time (Doi et al. 2021). Note that in some studies, polymers with short dense brushes on both ends of a linear backbone are called dumbbell polymers (Houli et al. 2002, Stadler et al. 2011), but they are different from the dumbbell polymers we focus on in this study. For the blend sample of a dumbbell-shaped polymer with an entangled linear chain, it is expected that the dumbbell molecule becomes a pseudo-entangled cross-linker with a longer characteristic time than the conventional entangled chains due to the penetration of the linear chain into the two distant ring sections separated via the central linear chain in the dumbbell polymer. However, there are no such experimental examples in the past, and hence the validity of the above hypothesis has not been confirmed.

In this study, therefore, dynamic viscoelastic measurements are performed on samples of entangled linear polymers blended with a ring polymer with relatively low molecular weight ($M_R \simeq 1.8\ M_e$) and a dumbbell-shaped polymer with the rings connected at both ends of a linear chain ($M_L \simeq 4.7\ M_e$). The effects of the addition of the ring and dumbbell polymers on the terminal relaxation behavior of the entangled linear polymers are discussed.

Experimental

L430 (Tosoh Co., Ltd.), which has a weight-average molecular weight M_w of 427 kg/mol, was used as an entangled linear PS sample. The entanglement molecular weight, M_e, of linear PS is known as 18.0 kg/mol (Ferry 1980), and hence L430 has an entanglement number $Z = M_w/M_e \simeq 24$. The synthesis of the dumbbell-shaped PS, D308030, as well as its constituents linear L80 and ring R30, was reported previously (Doi et al. 2016). The molecular characteristics of the samples are summarized in Table 1. Blend samples of L430 with L80, R30, or D308030 were prepared by freeze-drying of mixed dilute solutions as reported previously (Doi et al. 2015b). Here, L80 and D308030 were weighted to be equimolar to L430, while R30 was weighted to be double molar to L430. This mixing ratio was determined so that D308030 was present in equimolar to L430 in the L430/D308030 blend as a standard and that the linear and ring chains in the other blends correspond to the number of moles of the constituents in D308030 (i.e., one linear and two ring units). The volume fraction of L430, Φ_L, in the blend samples, which assumes that all components have the same density, is summarized in Table 2. After freeze-drying, the powder samples were subjected to thermal annealing in vacuum to make disk-shaped samples for rheological measurements.

Dynamic viscoelasticity measurements under linear strain were performed using an ARES-G2 rheometer (TA Instruments) under the same measurement conditions as in the past (Doi et al. 2015a, 2015b). Basically, a cone and plate geometry with 8 mm diameter was used, but due to the limited

Table 1 Molecular characteristics of the samples

Samples	M_w / kg mol^{-1}	M_w/M_n	Purity / %
L430[a]	427	1.02	-
L80[b]	84.0	1.06	-
R30[b]	33.7	1.02	99.9
D308030[b]	147	1.01	99.9

[a]Reported commercially; [b]reported previously in Doi et al. (2016).

Table 2 Characteristic rheological parameters of the samples

Samples	Φ_L [a]	$10^{-5}\ \eta_0$ / Pa s	$10^5\ J_e^\circ$ / Pa^{-1}
L430	1	$68._2$	1.2_8
L430/L80	0.84	$47._1$	1.3_1
L430/R30	0.86	$62._6$	1.3_1
L430/D308030	0.74	$125._0$	1.4_9

[a] Φ_L is estimated under assumption that the density of all components (i.e., L430, L80, R30, and D308030) is equal.

sample volume, 4 mm diameter parallel plate geometry was used for the L430/D308030 blend. The data consistency for the two geometries has been confirmed from the measurements for standard polystyrene samples. The measurements were performed in the range of temperature $T = 160 \sim 240$ °C with a linear strain amplitude of less than 5%.

Results and discussion

Figure 1 shows the master curves of storage and loss moduli (G' and G'', respectively) and tan δ ($=G''/G'$) for L430, L430/L80, and L430/R30, while Fig. 2 compares those for L430 and L430/D308030 at the reference temperature $T_r = 160$ °C. Figure 3 displays the temperature dependence of horizontal shift factors a_T so as to construct the master curves for all the samples, being evident that the blend samples exhibit a temperature dependence of a_T expressed

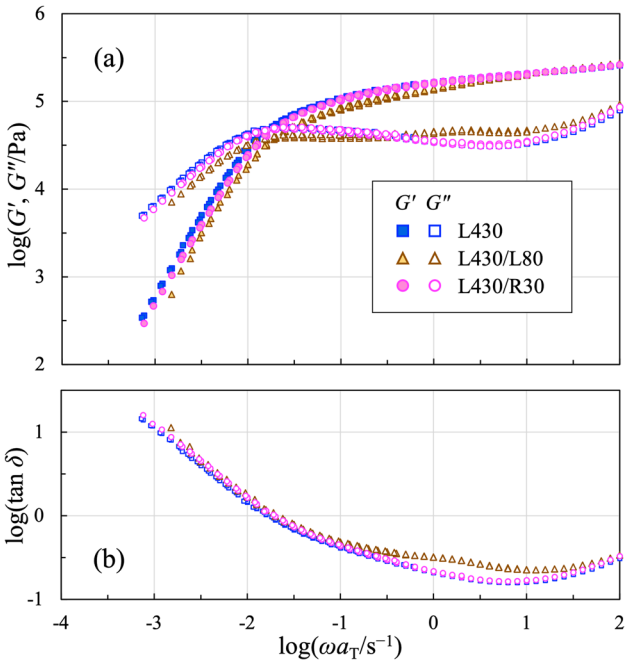

Fig. 1 Master curves of **a** G', G'' and **b** tan δ for L430, L430/L80, and L430/R30, reduced at $T_r = 160$ °C

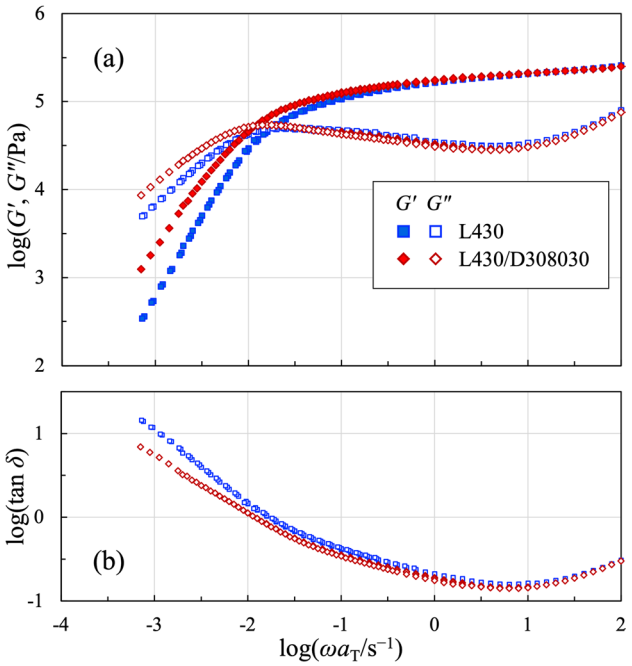

Fig. 2 Master curves of **a** G', G'' and **b** tan δ for L430 and L430/D308030 reduced at $T_r = 160$ °C

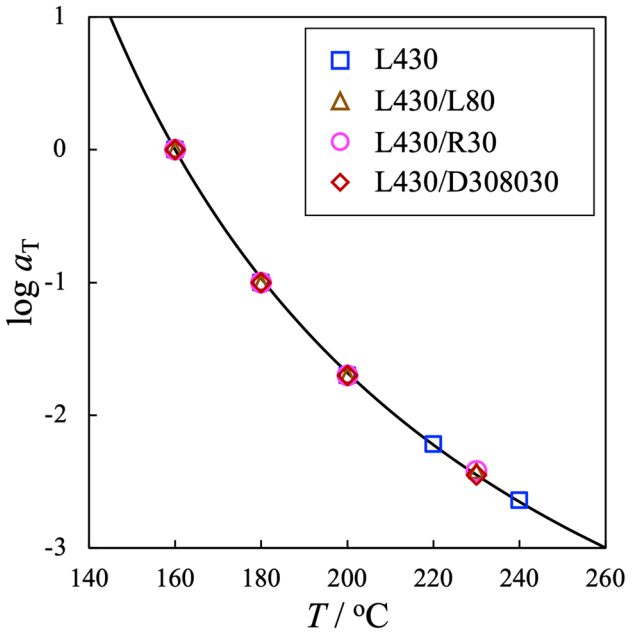

Fig. 3 Temperature dependence of horizontal shift factors a_T for the samples at $T_r = 160$ °C

as $\log a_T = -6.3(T - T_r)/(110 + T - T_r)$, which is consistent with that of L430 and other linear PS reported previously (Doi et al. 2015b, 2020). The dynamic modulus measured at each T in Figs. 1 and 2 was corrected by shifting along the vertical axis by $b_T = \rho(T_r)T_r/\rho(T)T$ where $\rho(T)$ is the density

of PS at T described by an empirical equation, $\rho(T) = 1.2503 - 6.50 \times 10^{-4}$ T (ρ in g cm^{-1} and T in K; Zoller and Walsh 1995). In addition, van Gurp-Palmen plot (i.e., the absolute value of the complex modulus $|G^*| = \{(G')^2 + (G'')^2\}^{1/2}$ vs phase angle δ; van Gurp and Palmen 1998) of the samples is shown in Fig. 5 in Appendix.

Figure 1a shows that $G^*(\omega)$ of the two blends, L430/L80 and L430/R30, overlaps well with that of L430 at the high ω limit (i.e., $\omega a_T = 10^2$ s^{-1}). The plateau modulus G_N for the blends estimated from the G' value at the minimum point of tan δ is also in good agreement with that of L430, i.e., 2×10^5 Pa, within the error range. In contrast, in the low to middle ω range ($10^{-3} \sim 10^1$ s^{-1}), $G^*(\omega)$ is different among the samples. That is, G' in the plateau region decays faster and G' and G'' in the terminal region ($\omega a_T = 10^{-3} \sim 10^{-2}$ s^{-1}) is lower in the order of L430/L80, L430/R30, and L430. Two rheological parameters that characterize the terminal relaxation behavior, i.e., zero-shear viscosity η_0 ($= \lim_{\omega \to 0}\{G''(\omega)/\omega\}$) and steady-state recoverable compliance J_e^o ($= (1/\eta_0^2)\lim_{\omega \to 0}\{G'(\omega)/\omega^2\}$), are estimated, and the values obtained are summarized in Table 2. Qualitatively, η_0 increases in the order of L430/L80, L430/R30, and L430, while J_e^o, which represents the relaxation mode distribution, is almost the same among L430, L430/L80, and L430/R30, but that for L430/D308030 is slightly higher than the others. The molecular weight dependence of η_0 is shown in Fig. 6 in Appendix, in order to discuss the extent of the difference in η_0 values between the samples.

From Fig. 1b, the difference in the shape of tan δ shows the difference in relaxation modes between L430, L430/R30, and L430/L80. That is, L430 and L430/R30 essentially exhibit a one-step relaxation with a minimum tan δ at around $\omega a_T = 10^{0.8}$ s^{-1}, whereas L430/L80 exhibits two minima of tan δ at around $\omega a_T = 10^{1.0}$ s^{-1} and $10^{-0.4}$ s^{-1}, indicating the latter possesses two different relaxation origins. There have been several reports on the linear viscoelastic properties of binary linear polymer blends with different molecular weights (Watanabe 1999; Read et al. 2012, 2018), where it is well-established that the low molecular weight component relaxes first, followed by the relaxation of high molecular weight component. Figure 4b shows a schematic illustration of the entangled linear polymer blend L430/L80 compared to that of entanglement for the neat L430 in Fig. 4a.

In contrast, tan δ of the L430/R30 blend is similar to that of the neat L430. If R30, which originally has a much faster relaxation time, relaxes independently from L430, L430/R30 would exhibit a two-step relaxation as observed in L430/L80. However, the L430/R30 blend exhibits a one-step relaxation, which could be due to the incorporation of R30 into the entanglement network of L430. In other words, R30 may be spontaneously penetrated by L430 and adopt the conformation as schematically shown in Fig. 4c. In fact, viscoelasticity data have been obtained for tadpole- and

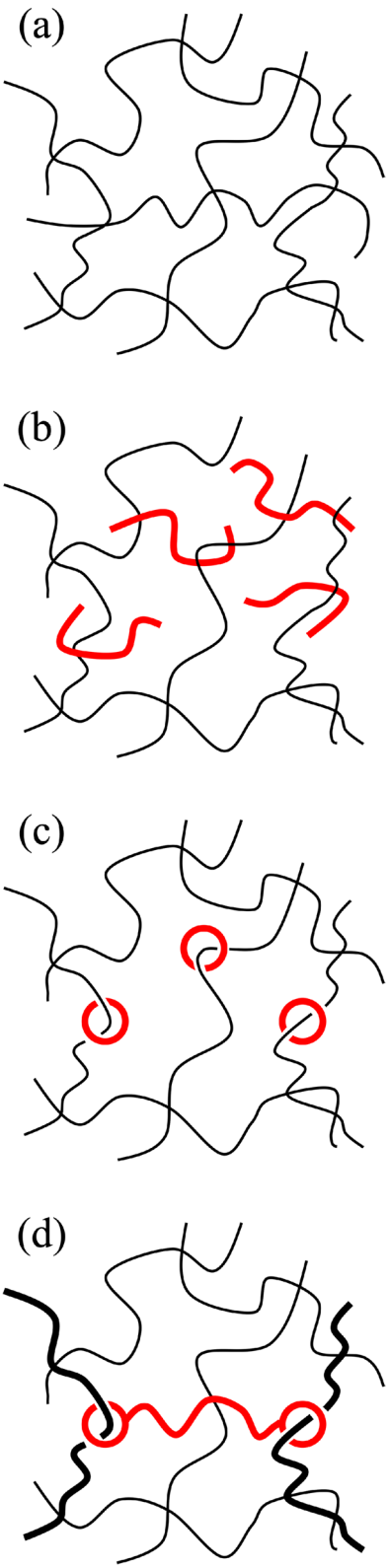

Fig. 4 Schematic illustration of entangled polymer chains for **a** L430, **b** L430/L80, **c** L430/R30, and **d** L430/D308030

dumbbell-shaped polymers having R30 as a constituent, suggesting that R30 is spontaneously penetrated by other molecules in melts (Doi et al. 2020, 2021). This experimental fact is consistent with the present molecular picture in Fig. 4c.

In some previous studies, η_0 of ring/linear polymer blends was evidently higher than that of the component linear neat polymers (Kapnistos et al. 2008; Parisi et al. 2020; Kong et al. 2022). In those studies, both linear and ring polymers have sufficiently higher molecular weights ($M_L \simeq M_R \simeq 10M_e$), where it can be considered that several linear chains spontaneously penetrate into one ring. As a result, the motion of the rings was heavily constrained by the penetrating linear chains. In other words, the constraint release (CR) could be the primary relaxation mechanism for the rings penetrated/entangled by the surrounding linear chains, as proposed previously (Parisi et al. 2020). Correspondingly, the occurrence of the CR process in the entangled linear chains, which penetrate the rings, may also decrease in the ring/linear blends. In contrast, η_0 of the L430/R30 blend examined in this study is just slightly lower than that of neat L430. This result suggests that the underlying physics in L430/R30 is different from the ring/linear blends with large rings in the previous studies. Although a detailed molecular picture cannot be described merely from the present viscoelastic data, we consider that the ring must be large enough to allow multiple linear chain penetrations to delay terminal relaxation of the ring/linear blend systems, just like a pseudo entanglement cross-linker. It can be assumed in the L430/R30 blend that a threading of multiple linear chains into one ring does not frequently occur due to the small size of R30, and hence, the ring does not act as a pseudo entanglement cross-linker. In order to elucidate the viscoelastic behavior and molecular picture of ring/linear blends, further measurements of systematic samples using rings with different molecular weights and also different ring/linear fractions are needed in the future.

Finally, we focus on the viscoelastic behavior of the linear/dumbbell-shaped polymer blend. Figure 2a shows that G' of L430/D308030 is almost the same as that of neat L430 in the plateau region at $\omega a_T = 10^{-1} \sim 10^2$ s^{-1}. On the other hand, in the terminal region of $\omega a_T \leq 10^{-1}$ s^{-1}, G' and G'' of L430/D308030 are evidently higher than those of L430. Table 2 shows that η_0 and J_e^o of L430/D308030 are higher than those of L430, which is a clearly different trend from the L430/L80 and L430/R30 blends.

From Fig. 2b, tan δ of L430/D308030 has basically one minimum, and its relaxation behavior is similar to that of L430 and L430/R30. That is, the ring parts in D308030 is considered to be incorporated in the entanglement network of L430 like R30 in the L430/R30 blend, as schematically shown in Fig. 4d. This molecular picture reminds us of slide-ring gels (Okumura and Ito 2001; Mayumi and Ito 2010). One particular difference from the L430/R30 blend is that the two R30 sections in D308030 are separated via a central linear chain L80, which may act as a pseudo-entanglement point. In L430/D308030, there are three possible mechanisms for D308030, as CR (as with large rings in ring/linear blends, if both ring parts at the ends are penetrated by L430), arm retraction (if one of the rings is free from linear chain threading), and reptation (if both rings are free). As for the reptation, it would not be a very frequent event in this case, judging from the comparison of the viscoelastic data for L430/D308030 and L430/L80. In order to estimate the contribution of arm retraction, it would be useful to look at the viscoelastic data of a blend of L430 and a single-tail tadpole-shaped polymer S3080 where R30 is attached at only one end of L430. The data is shown in Fig. 7 in Appendix. As detailed in Appendix, the terminal relaxation behavior of L430/S3080 is similar to that of L430/R30 (although there is a difference between them in the middle ω range), and hence, L430/D308030 exhibits slower terminal relaxation than L430/S3080. The above experimental facts support that the CR mechanism is the main contribution in the relaxation mode of D308030 in the L430/D308030 blend. Correspondingly, D308030 does not allow the CR motion of a part of entangled L430 chains. The slower and broader terminal relaxation seen at $\omega a_T \leq 10^{-2}$ s^{-1} (which corresponds to a slightly higher η_0 and J_e^o values than neat L430) can also be attributed to this molecular picture. One might wonder how the molecular weight of the linear and ring parts of dumbbell molecules affects the viscoelastic behavior of linear/dumbbell polymer blends. At present, we have only one data shown in Fig. 2, and thus, it is difficult to correctly discuss the role of molecular weight in the dumbbell molecule. However, based on the above discussion, we can infer that the length of the central linear chain section is not so important, but rather the presence of two ring parts that can allow linear chain penetration in dumbbell molecules. In this respect, we need further experiments using dumbbell samples with different molecular weight of the ring and linear sections in the future.

Conclusions

In this study, we investigated the effect of the addition of R30 and D308030 to the entangled linear polymer L430 on the terminal relaxation behavior. When R30 was blended with L430, the blend exhibited a one-step terminal relaxation behavior, which is clearly different from that of binary linear chain blends with different molecular weights. η_0 of the L430/R30 blend is lower than that of neat L430, which is qualitatively different from the results of large ring/linear blends reported previously. These results suggested that the penetration of multiple linear chains into R30 does

not frequently occur and simply reduced the entanglement concentration of L430 slightly. The L430/D308030 blend exhibited higher η_0 and J_e^o than L430, unlike the L430/R30 blend. This result suggests that the two ring sections in the dumbbell molecule separated by the central linear chain were spontaneously penetrated by the L430 chains, and the dumbbell chain acts as a pseudo-entanglement point with a longer characteristic time.

Appendix

Figure 5 shows the van Gurp-Palmen (vGP) plot (i.e., the absolute value of the complex modulus $|G^*| = \{(G')^2 + (G'')^2\}^{1/2}$ vs phase angle δ; van Gurp and Palmen 1998) for L430/D30/80/30 compared with those for L430, L430/L80, and L430/R30 at $T_r = 160$ °C. The vGP-plot is known to be sensitive to the differences in molecular architecture and molecular weight distribution of the samples (Trinkle and Friedrich 2001; Trinkle et al. 2002; Qian and McKenna 2018). We can see from Fig. 5 that time–temperature superposition (TTS) is hold for all the samples examined in this study, as confirmed in Figs. 1 and 2 in the main text. Compared to L430, L430/L80 clearly shows a different vGP plot shape, which is due to the fact that L430 and L80 relax separately on different time scales, as confirmed in Fig. 1 in the main text. In contrast, L430/R30 and L430/D308030 exhibit vGP plot apparently similar to those of L430. A more careful look at Fig. 5 reveals that the L430/D308030 blend shows a more gradual increase in δ with respect to the decrease in $|G^*|$. This result corresponds to the fact that L430/D308030 exhibits a broader terminal relaxation than L430.

Figure 6 shows the molecular weight dependence of η_0 for linear PS samples reported by various researchers (Doi et al. 2015a; Roovers 1985; McKenna et al. 1989; Plazek and O'Rourke 1971; Montfort et al. 1984). As is well known, η_0 increases in proportion to M_w in the M_w range below the critical molecular weight $M_c \simeq 2M_e = 36.0$ kg/mol, while η_0 shows a dependence on $M_w^{3.4}$ at M_w above M_c (Ferry 1980). We also plotted η_0 for the series of blend samples examined in this study at $M_w = 427$ kg/mol. Although there is some variation in the reported η_0 values of linear PSs, the η_0 of L430/D308030 in this study is considerably higher than that of L430 in Fig. 6.

Figure 7 shows G', G'' and tan δ for L430/S3080 compared with those for L430, L430/L80 and L430/R30 at $T_r = 160$ °C. Note that S3080 indicates the single-tail tadpole-shaped PS, which was obtained in the synthesis process of D308030 as reported previously (Doi et al. 2016). The temperature dependence of a_T of L430/S3080 is exactly the same with that of other blends as well as L430. Figure 7 shows that $G^*(\omega)$ in the high ω limit (i.e., $\omega a_T = 10^2$ s^{-1})

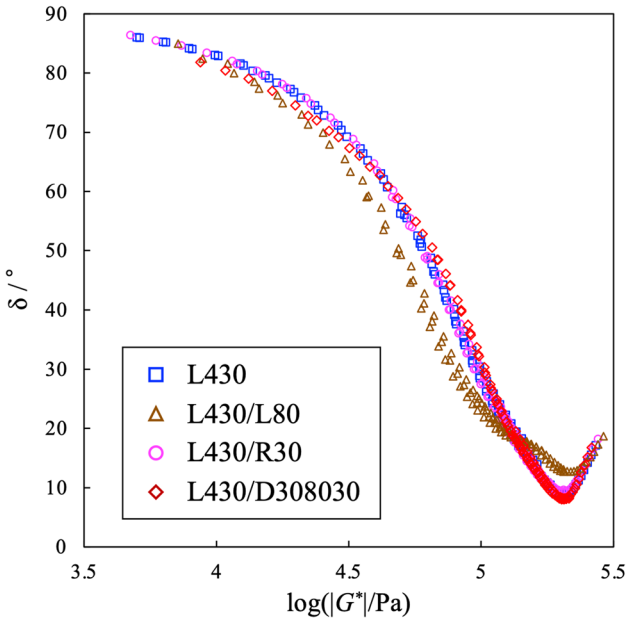

Fig. 5 van-Gurp-Palmen plot of L430, L430/L80, L430/R30, and L430/D308030 reduced at $T_r = 160$ °C.

agrees well with that of L430 and other blends. The terminal relaxation behavior of L430/S3080 at $\omega a_T \leq 10^{-1}$ s^{-1} is also in good agreement with that of L430/R30. On the other hand, there is a difference between L430/S3080 and the other blends in the middle ω region of $10^{-1} \leq \omega a_T / \text{s}^{-1} \leq 10^1$. That is, in this ω range, there is no difference in G' between

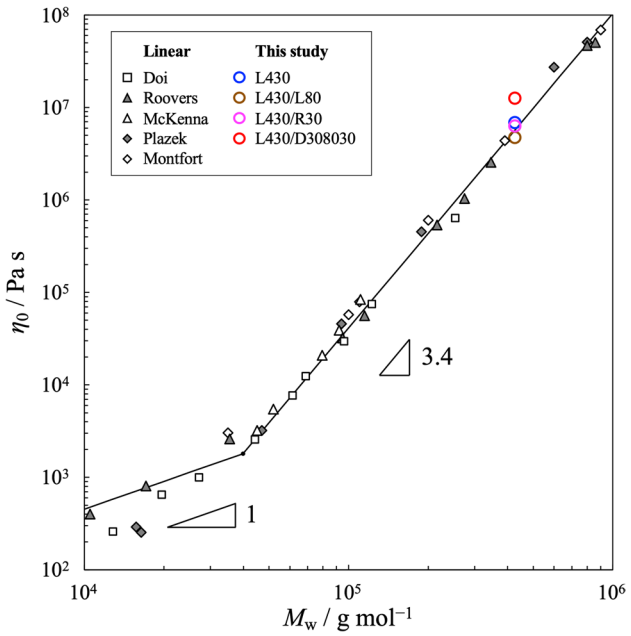

Fig. 6 Molecular weight dependence of η_0 for linear PS samples (Doi et al. 2015a; Roovers 1985; McKenna et al. 1989; Plazek and O'Rourke 1971; Montfort et al. 1984) compared with that for L430/L80, L430/R30, and L430/D308030 at $T_r = 160$ °C

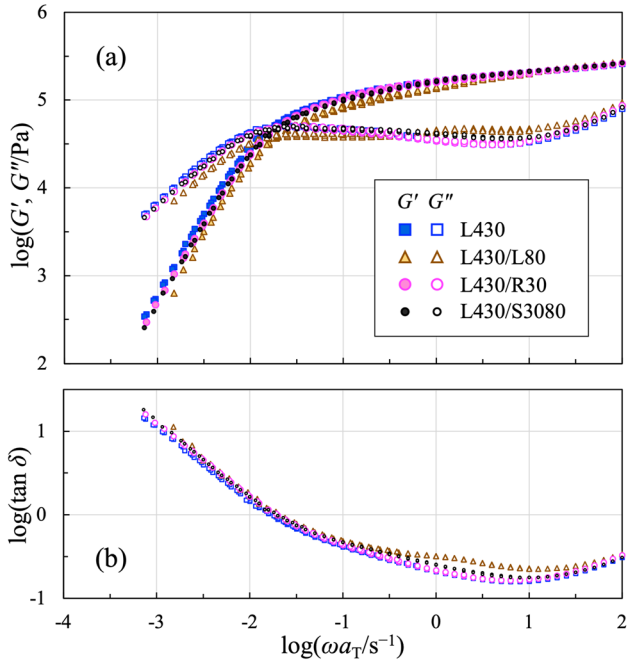

Fig. 7 Master curves of **a** G', G'' and **b** tan δ for L430, L430/L80, and L430/R30 and L430/S3080, reduced at $T_r = 160$ °C

the samples, while G'' of L430/S3080 is higher than that of L430 and L430/R30, but lower than that of L430/L80. Based on the results in the main text, it is expected that the ring part in S3080 is also penetrated by L430. Therefore, in the middle ω range, the linear tail part of S3080 can be relaxed, but the whole S3080 molecule cannot be relaxed due to the ring part bounded by the penetration.

Acknowledgements The authors acknowledge Prof. Hiroshi Watanabe at Kyoto University and Prof. Yuichi Masubuchi at Nagoya University for their helpful discussion. The authors acknowledge Prof. Tadashi Inoue at Nagoya University for providing us with the 4 mm diameter parallel plate geometry for rheological measurements.

Funding This work was partly supported by JSPS KAKENHI Grant Numbers 21K14682 for Y.D., 24350056 for A.T., and 25248048 for Y.M.

Declarations

Competing interest The authors declare no competing interests.

References

Borger A, Wang W, O'Connor TC, Ge T, Grest GS, Jensen GV, Ahn J, Chang T, Hassager O, Mortensen K, Vlassopoulos D, Huang Q (2020) Threading-unthreading transition of linear-ring polymer blends in extensional flow. ACS Macro Lett 9:1452–1457

Doi Y, Matsubara K, Ohta Y, Nakano T, Kawaguchi D, Takahashi Y, Takano A, Matsushita Y (2015) Melt rheology of ring polystyrenes with ultrahigh purity. Macromolecules 48:3140–3147

Doi Y, Takano A, Takahashi Y, Matsushita Y (2015) Melt rheology of tadpole-shaped polystyrenes. Macromolecules 48:8667–8674

Doi Y, Takano A, Matsushita Y (2016) Synthesis and characterization of dumbbell-shaped polystyrene. Polymer 106:8–13

Doi Y, Matsumoto A, Inoue T, Iwamoto T, Takano A, Matsushita Y, Takahashi Y, Watanabe H (2017) Re-examination of terminal relaxation behavior of high-molecular-weight ring polystyrene melts. Rheol Acta 56:567–581

Doi Y, Takano A, Takahashi Y, Matsushita Y (2020) Melt rheology of tadpole-shaped polystyrene with different ring sizes. Soft Matter 16:8720–8724

Doi Y, Takano A, Takahashi Y, Matsushita Y (2021) Viscoelastic properties of dumbbell-shaped polystyrenes in bulk and solution. Macromolecules 54:1366–1374

Doi Y (2022) Rheological properties of ring polymers and their derivatives. Nihon Reoroji Gakk (J Soc Rheol Jpn) 50:7–62

Ferry JD (1980) Viscoelastic properties of polymers. John Wiley and Sons, New York

Ge T, Panyukov S, Rubinstein M (2016) Self-similar conformations and dynamics in entangled melts and solutions of nonconcatenated ring polymers. Macromolecules 49:708–722

Goossen S, Kruteva M, Sharp M, Feoktystov A, Allgaier J, Pyckhout-Hintzen W, Wischnewski A, Richter D (2015) Sensing polymer chain dynamics through ring topology: a neutron spin echo study. Phys Rev Lett 115:148302

Hagita K, Murashima T (2021) Molecular dynamics simulations of ring shapes on a ring fraction in ring-linear polymer blends. Macromolecules 54:8043–8051

Halverson JD, Lee WB, Grest GS, Grosberg AY, Kremer K (2011) Molecular dynamics simulation study of nonconcatenated ring polymers. I Statics J Chem Phys 134:204904

Halverson JD, Grest GS, Grosberg AY, Kremer K (2012) Rheology of ring polymer melts: from linear contaminants to ring-linear blends. Phys Rev Lett 108:038301

Houli S, Iatrou H, Hadjichristidis N, Vlassopoulos D (2002) Synthesis and viscoelastic properties of model dumbbell copolymers consisting of a polystyrene connector and two 32-arm star polybutadiene. Macromolecules 35:6592–6597

Iwamoto T, Doi Y, Kinoshita K, Ohta Y, Takano A, Takahashi Y, Nagao M, Matsushita Y (2018) Conformation of ring polystyrenes in bulk studied by SANS. Macromolecules 51:1539–1548

Iwamoto T, Doi Y, Kinoshita K, Takano A, Takahashi Y, Kim E, Kim TH, Takata S, Nagao M, Matsushita Y (2018) Conformation of ring polystyrenes in semidilute solutions and in linear polymer matrices studied by SANS. Macromolecules 51:6836–6847

Iyer BVS, Lele AK, Shanbhag S (2007) What is the size of ring polymer in a ring-linear blend? Macromolecules 40:5995–6000

Kapnistos M, Lang M, Vlassopoulos D, Pyckhout-Hintzen W, Richter D, Cho D, Chang T, Rubinstein M (2008) Unexpected power-law stress relaxation of entangled ring polymers. Nat Mater 7:997–1002

Kong D, Banik S, San Francisco BM, Lee M, Robertson-Anderson RM, Schroeder CM, McKenna GB (2022) Rheology of entangled solutions of ring-linear DNA blends. Macromolecules 55:1205–1217

Kruteva M, Allgaier J, Richter D (2017) Direct observation of two distinct diffusive modes for polymer rings in linear polymer matrices by pulsed field gradient (PFG) NMR. Macromolecules 50:9482–9493

Kruteva M, Monkenbusch M, Allgaier J, Holderer O, Pasini S, Hoffmann I, Richter D (2020) Self-similar dynamics of large rings: a neutron spin echo study. Phys Rev Lett 125:238004

Kruteva M, Allgaier J, Monkenbusch M, Porcar L, Richter D (2020) Self-similar polymer ring conformations based on elementary loop: a direct observation by SANS. ACS Macro Lett 9:507–511

Lee HC, Lee H, Lee W, Chang T, Roovers J (2000) Fractionation of cyclic polystyrene from linear precursor by HPLC at the chromatographic critical condition. Macromolecules 33:8119–8121

Mayumi K, Ito K (2010) Structure and dynamics of polyrotaxane and slide-ring materials. Polymer 51:959–967

McKenna GB, Hostetter BJ, Hadjichristidis N, Fetters LJ, Plazek DJ (1989) A study of the linear viscoelastic properties of cyclic polystyrenes using creep and recovery measurements. Macromolecules 22:1834–1852

Montfort JP, Marin G, Monge P (1984) Effects of constraint release on the dynamics of entangled linear polymer melts. Macromolecules 17:1551–1560

Nam S, Leisen J, Breedveld V, Beckham HW (2009) Melt dynamics of blended poly(oxyethylene) chains and rings. Macromolecules 42:3121–3128

Obukhov SP, Rubinstein M, Duke T (1994) Dynamics of a ring polymer in a gel. Phys Rev Lett 73:1263–1266

Okumura Y, Ito K (2001) The polyrotaxane gels: a topological gel by figure-of-eight cross-links. Adv Mater 13:485–487

Parisi D, Ahn J, Chang T, Vlassopoulos D, Rubinstein M (2020) Stress relaxation in symmetric ring-linear polymer blends at low ring fractions. Macromolecules 53:1685–1693

Plazek DJ, O'Rourke VM (1971) Viscoelastic behavior of low molecular weight polystyrene. J Polym Sci Part A-2: Polym Phys 9:209–243

Qian Z, McKenna GB (2018) Expanding the application of the van Gurp-Palmen plot: new insights into polymer melt rheology. Polymer 155:208–217

Read DJ, Jagannathan K, Sukmaran SK, Auhl D (2012) A full-chain constitutive model for bidisperse blends of linear polymers. J Rheol 56:823–873

Read DJ, Shivokhin ME, Likhtman AE (2018) Contour length fluctuations and constraint release in entangled polymers: slop-spring simulations and their implications for binary blend rheology. J Rheol 62:1017–1036

Richter D, Goossen S, Wischnewski A (2015) Celebrating Soft Matter's 10th anniversary: topology matters: structure and dynamics of ring polymers. Soft Matter 11:8535–8549

Robertson RM, Smith DE (2007) Self-diffusion of entangled linear and circular DNA molecules: dependence on length and concentration. Macromolecules 40:3373–3377

Roovers J (1985) Viscoelastic properties of ring polystyrenes. Macromolecules 18:1359–1361

Stadler FJ, Rajan M, Agarwal US, Liu CY, George KE, Lemstra PJ, Bailly C (2011) Rheological characterization in shear of a model dumbbell polymer concentrated solution. Rheol Acta 50:491–501

Subramanian G, Shanbhag S (2008) Conformational properties of blends of cyclic and linear polymer melts. Phys Rev E 77:011801

Suzuki J, Takano A, Deguchi T, Matsushita Y (2009) Dimension of ring polymers in bulk studied by Monte-Carlo simulation and self-consistent theory. J Chem Phys 131:144902

Trinkle S, Friedrich C (2001) Van Gurp-Palmen-plot: a way to characterize polydispersity of linear polymers. Rheol Acta 40:322–328

Trinkle S, Walter P, Friedrich C (2002) Van Gurp-Palmen plot II – classification of long chain branched polymers by their topology. Rheol Acta 41:103–113

Tsalikis DG, Mavrantzas VG (2014) Threading of ring poly(ethylene oxide) molecules by linear chains in the melt. ACS Macro Lett 3:763–766

Tsalikis DG, Mavrantzas VG (2020) Size and diffusivity of polymer rings in linear polymer matrices: the key role of threading events. Macromolecules 53:803–820

Van Gurp M, Palmen J (1998) Time temperature superposition for polymeric blends. Rheol Bull 67:5–8

Vlassopoulos D (2016) Molecular topology and rheology: beyond the tube model. Rheol Acta 55:613–632

Watanabe H (1999) Viscoelasticity and dynamics of entangled polymers. Prog Polym Sci 24:1253–1403

Young CD, Zhou Y, Schroeder CM, Sing CE (2021) Dynamics and rheology of ring-linear blend semidilute solutions in extensional flow. Part I: modeling and molecular simulations. J Rheol 65:757–777

Zhou Y, Hsiao KW, Regan KE, Kong D, McKenna GB, Robertson-Anderson RM, Schroeder CM (2019) Effect of molecular architecture on ring polymer dynamics in semidilute linear polymer solutions. Nat Commun 10:1753

Zhou Y, Young CD, Lee M, Banik S, Kong D, McKenna GB, Robertson-Anderson RM, Sing CE, Schroeder CM (2021) Dynamics and rheology of ring-linear blend semidilute solutions in extensional flow: Single molecule experiments. J Rheol 65:729–744

Zoller P, Walsh D (1995) Standard pressure-volume-temperature data for polymers. Technomic Pub, Lancaster